

doi: 10.13241/j.cnki.pmb.2018.15.028

## 宝石能谱 CT GSI 成像和常规成像在上腹部应用价值的对比研究

徐汝建 康 露 向映光 李亚林 李 毅

(广元市中心医院医学影像科 四川 广元 628000)

**摘要** 目的:探讨宝石能谱 CT GSI 扫描模式在上腹部检查中降低辐射剂量和优化图像质量的可行性及应用价值。方法:选择 2016 年 9 月至 2016 年 12 月期间我院 40 例拟行上腹部三期增强的患者,根据扫描模式将患者分为 A 组和 B 组,每组 20 例。A 组患者采用宝石能谱 CT 常规扫描模式行螺旋扫描,管电压 120 Kvp 及自动毫安管电流,确定 NI 值为 10。B 组患者采用 GSI 模式行三期增强扫描收集门脉期图像。回顾性自适应统计迭代重建(ASIR)70kev 单能量图像,应用 ASIR Review 工具收集 0 到 100%ASIR 的 CT 值、噪声值,计算图像信号噪声比(SNR)。记录各组剂量报告中 CT 剂量容积指数(CTDI vol)及剂量长度乘积(DLP),并计算有效剂量(ED),采用图像质量主观评分对图像进行评价。结果:B 组 CT 值、噪声值及 SNR 均高于 A 组( $P<0.05$ ),B 组 CTDIvol、DLP 和 ED 均显著低于 A 组( $P<0.05$ );随着 ASIR 升高,SNR 升高,但是图像质量主观评分先升高后降低。当 ASIR 为 50% 时,图像质量最高,不同 ASIR 的 CT 值、噪声值之间的差异无统计学意义( $P>0.05$ )。结论:宝石能谱 CT GSI 扫描模式的效果明显优于螺旋扫描,同时在降低图像噪声的前提下选择 50%ASIR,可保障图像质量。

**关键词:**低辐射剂量;自适应统计迭代重建;ASIR Review 工具

中图分类号:R814.42;R57 文献标识码:A 文章编号:1673-6273(2018)15-2930-04

## Comparative Study of Gemstone Spectrum CT GSI Imaging and Conventional Imaging in Upper Abdominal Application Value

XU Ru-jian, KANG Lu, XIANG Ying-guang, LI Ya-lin, LI Yi

(Department of Medical Imaging, Guangyuan Central Hospital, Guangyuan, Sichuan, 628000, China)

**ABSTRACT Objective:** To explore the feasibility and application value of the gemstonespectrum CT GSI scanning mode in reducing the radiation dose and optimizing image quality in the upper abdominal examination. **Methods:** A total of 40 patients, who underwent upper abdominal three stage enhancement in Guangyuan Central Hospital during September 2016 to December 2016, were selected and divided into group A(n=20) and group B(n=20) according to the scan mode. Group A was performed spiral scanning by gemstone spectrum CT conventional scanning mode (tube voltage: 120Kvp; tube current of automatic milliampere; NI value:10). Group B was performed three stage enhanced scanning by GSI mode to collect portal phase image. ASIR CT values and noise values from 0 to 100% were collected by ASIR Review tool [retrospective adaptive statistical iterative reconstruction (ASIR)70kev single energy image]. The image signal to noise ratio (SNR) was calculated. The CT dose volume index (CTDI vol) and dose length product (DLP) were recorded in each dose report, and the effective dose (ED) was calculated. The images were evaluated according to image subjective scores. **Results:** The CT value, noise value and SNR of group B were higher than those of group A ( $P<0.05$ ). The CTDIvol, DLP and ED of group B were significantly lower than those of group A ( $P<0.05$ ). With the increase of ASIR, the SNR increased, but subjective score of image quality increased at first and then decreased. When ASIR was 50%, the image quality was the best. There were no statistical differences in CT value and noise value between different ASIR, and noise value ( $P>0.05$ ). **Conclusion:** The effect of gemstone spectrum CT GSI scanning mode is significantly better than spiral scanning. At the same time, under the premise of reducing the image noise, selecting 50% ASIR can ensure the image quality.

**Key words:** Low radiation dose; Adaptive statistical iterative reconstruction; ASIR Review tool

**Chinese Library Classification(CLC): R814.42; R57 Document code: A**

**Article ID:** 1673-6273(2018)15-2930-04

### 前言

医学成像占到人体所受辐射剂量的 50%,其中 CT 检查成为主要因素<sup>[1]</sup>。CT 扫描所致的辐射剂量受到全社会及医务工作者和患者的普遍关注<sup>[2]</sup>。CT 扫描中能量成像研究从能量减影转

变为单能谱,低管电压及自动管电流调节(ATCM)低剂量 CT 扫描技术是近年来研究的热点,临床应用广泛<sup>[3,4]</sup>。自适应统计迭代重建(ASIR)技术的问世使扫描条件降低但不增加图像噪声成为可能<sup>[5]</sup>。宝石能谱 CT 可以优化传统 CT 成像的细节,使得 CT 值的单参数转变为多参数,混合能量成像变为单能量成像,从而避免由于伪影和容积效应产生的漏诊和误诊,最终提高对小病灶和多发病灶的诊断效果。宝石能谱 CT 技术主要是将 X 线在物质中的衰减系数转化为图像信息,对特异性组织

作者简介:徐汝建(1967-),男,大专,主管技师,从事能谱 CT 相关方面的研究,E-mail:bwiege@163.com

(收稿日期:2017-09-25 接受日期:2017-10-21)

进行鉴别,另外还可以对不同的脏器、同一脏器的不同病变类型及同一病变的不同病理分期进行对比分析,从而为临床诊断和治疗提供依据<sup>[6,7]</sup>。本研究采用宝石能谱 CT GSI 扫描模式并与常规扫描模式对比研究,旨在探讨能谱 CT 在上腹部扫描中降低患者辐射剂量的可行性及应用价值,现报道如下。

## 1 资料与方法

### 1.1 一般资料

选取 2016 年 9 月至 2016 年 12 月间在本院行上腹部多期增强扫描的患者 40 例,纳入标准:<sup>①</sup> 无 CT 扫描禁忌症;<sup>②</sup> 临床资料完整且依从性高;<sup>③</sup> 经患者及其家属同意,并签订知情同意书。排除标准:<sup>④</sup> 碘对比剂过敏史;<sup>⑤</sup> 严重甲状腺功能亢进者,严重心、肝、肾功能衰竭患者以及有哮喘病史者;<sup>⑥</sup> 精神意识障碍患者。按照检查方法的不同分为宝石能谱 CT 常规扫描模式行螺旋扫描(A 组)及 GSI 模式行三期增强扫描(B 组),每组各 20 例。本研究经医院伦理委员会审核通过。

### 1.2 方法

#### 1.2.1 扫描方法 使用 GE Discovery CT 750 HD 扫描仪对 A

组患者腹部行能谱常规平扫及 B 组患者腹部行多期增强能谱 GSI 扫描<sup>[8]</sup>,A、B 两组扫描范围高度一致。扫描参数:A 组常规扫描模式确定 NI 值为 10,管电压 120kvp,自动毫安秒管电流;B 组能谱 CT GSI 扫描模式,机架转速 0.6s、固定管电流 375 mA、螺距 1.375:1.55.00、准直器厚度 0.625 mm、重建层厚和层间距均为 1.25 mm,对比剂碘佛醇(320 mgI/mL),流速 2.5~3.0 mL/s,剂量为 1 mL/kg,经肘前静脉高压注射器团注,采用智能追踪扫描方式,腹主动脉监测触发阈值 130 HU,触发后行动脉期扫描,60 S 行门脉期扫描,120 S 行延迟期扫描。检查前禁食水 6~8 小时,扫描前 15~30 min 嘱咐患者饮清水 500~800 mL。

**1.2.2 图像后处理及数据收集** A 组常规扫描模式平扫图像采用 FBP 图像后重建,B 组 GSI 扫描模式采用 70 keV 回顾性重建图像,利用 ASIR Review 工具测量肝门附近层面肝右前叶、肝右后叶、肝方叶三处肝实质的 CT 值、噪声值,ROI 大小为(100±10)mm<sup>2</sup>(见图 1),求其平均值,计算图像信号噪声比(SNR)。记录由扫描仪提供的容积剂量指数(CTDI vol)及剂量长度乘积(DLP),计算有效辐射剂量(ED), $ED = DLP * 0.015^{[9]}$ 。

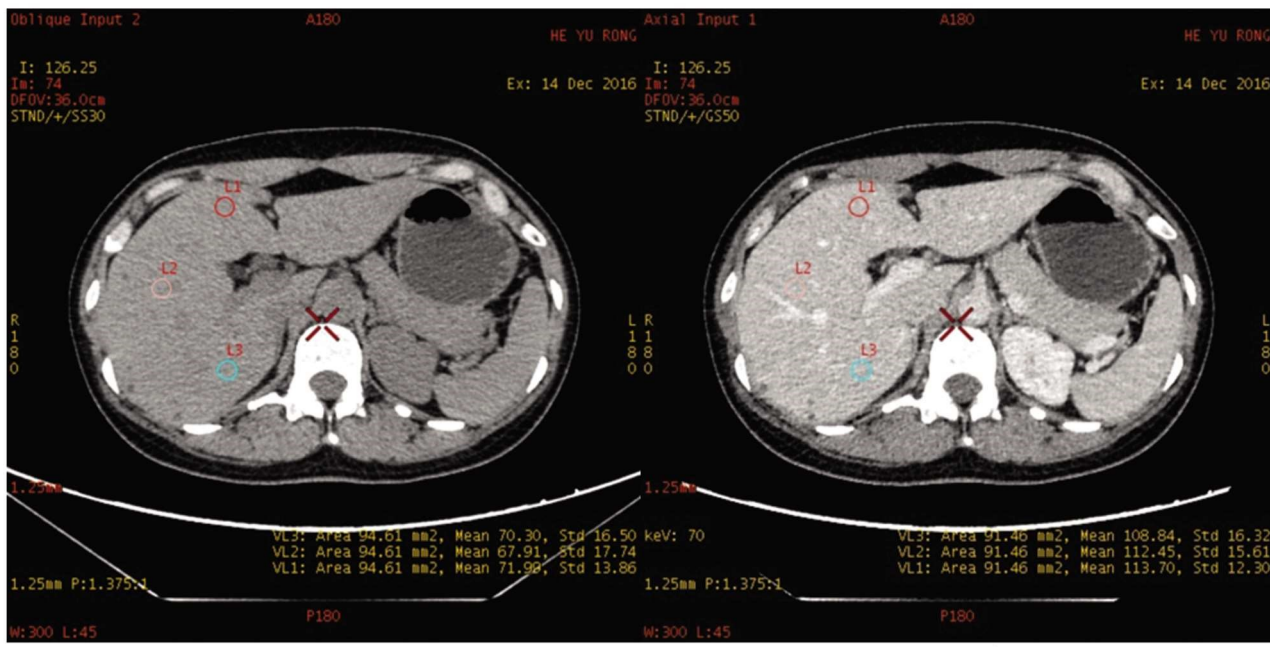


图 1a 常规扫描模式图像

Fig.1a Conventional scanning mode image

图 1b GSI 扫描模式图像

Fig.1b GSI scanning mode image

**1.2.3 图像质量评价** 图像质量主观评分标准(5 分):1 分:图像伪影或者噪声过大,无法诊断;2 分:图像的质量较差,且存在严重噪声或者伪影,对诊断有影响;3 分:质量一般,存在部分噪声或者伪影,但对诊断无明显影响;4 分:图像质量好,伪影及噪声均较少;5 分:图像的质量很好,无伪影,噪声抑制效果好。

### 1.3 统计学分析

使用 SPSS19.0 软件进行统计学分析。所有计量资料均符合正态分布,肝实质的 CT 值、噪声值、SNR 等计量资料采用均数±标准差( $\bar{x} \pm s$ )表示,均采用独立样本 t 检验。 $P < 0.05$  则认为差异具有统计学意义。

## 2 结果

### 2.1 两组一般资料比较

两组患者的性别、年龄及体质量指数(BMI)之间的差异无统计学意义( $P > 0.05$ ),如表 1 所示。

### 2.2 两组图像数据比较

B 组 CT 值、噪声值及 SNR 均高于 A 组,差异具有统计学意义( $P < 0.05$ )。B 组 CTDIvol、DLP 和 ED 均显著低于 A 组,差异具有统计学意义( $P < 0.05$ ),如表 2 所示。

**2.3 不同权重 ASIR 图像质量主观评分及 CT 值、噪声值、SNR 比较**

随着 ASIR 值升高, SNR 值升高,但是图像质量主观评分先升高后降低,当 ASIR 为 50% 时,图像质量最高。不同 ASIR

值之间的 CT 值、噪声值比较差异无统计学意义( $P>0.05$ ),如表 3 所示。

表 1 两组一般资料比较

Table 1 Comparison of general data between the two groups

Groups	Cases	Gender (Male/Female)	Age (years old)	BMI( $\text{kg}/\text{m}^2$ )
Group A	20	10/10	48.73± 6.21	23.15± 4.25
Group B	20	9/11	49.06± 6.33	23.26± 4.31
$\chi^2/t$		0.100	0.166	0.081
P		0.752	0.869	0.936

表 2 两组图像数据比较

Table 2 Comparison of two groups of image parameters

Groups	n	CT value	Noise value	SNR	CTDIvol(mGy)	DLP(mGy·cm)	ED(mGy)
Group A	20	67.91± 6.12	17.05± 1.99	4.04± 0.59	12.84± 3.80	421.93± 144.00	6.33± 2.16
Group B	20	101.51± 9.37	22.69± 3.90	4.60± 0.88	6.52± 0.00	212.30± 16.97	3.18± 0.25
t		13.428	5.761	2.364	7.438	6.466	6.479
P		0.000	0.000	0.023	0.000	0.000	0.000

表 3 不同权重 ASIR 图像质量主观评分及 CT 值、噪声值、SNR 比较

Table 3 Comparison of subjective score of image quality and CT value, noise value, SNR in Different weights of ASIR

Different ASIR value	Subjective score of image quality	CT value	Noise value	SNR
0	2.99± 0.08	101.52± 9.37	22.67± 3.91	4.60± 0.88
10%	3.16± 0.47	101.00± 9.44	21.57± 3.90	4.83± 0.95
20%	3.64± 0.61	101.06± 9.45	20.38± 3.81	5.12± 1.03
30%	4.38± 0.53	101.02± 9.45	19.23± 9.71	5.44± 1.12
40%	4.86± 0.30	101.17± 9.39	17.99± 3.63	5.84± 1.23
50%	4.91± 0.25	101.23± 9.47	16.94± 3.51	6.22± 1.36
60%	4.21± 0.48	101.10± 9.46	15.82± 6.43	6.68± 1.50
70%	3.61± 0.49	101.06± 9.47	14.72± 3.35	7.21± 1.69
80%	3.24± 0.42	101.12± 9.48	13.64± 3.26	7.82± 1.90
90%	3.10± 0.30	101.08± 9.48	12.63± 3.20	8.49± 1.90
100%	3.74± 0.81	101.78± 9.23	11.74± 3.07	9.26± 2.48

### 3 讨论

随着医学技术的发展,CT 技术已经问世 30 余年,能够快速、无创、直观地观察到肝部病变,对于治疗方案的确定和疗效评价具有重要作用<sup>[10,11]</sup>。传统 CT 成像技术使用包含不同能量的 X 线进行扫描,作用过程中高能段主要为康普顿效应,低能段主要为光电吸收<sup>[12-14]</sup>。X 线穿透身体时,低能量被滤掉,发生线束硬化效应,降低 CT 扫描的准确率,同时产生伪影,另外混合能量发生平均效应降低物质的对比度,从而降低固有信噪比,最终影响诊断效果<sup>[15]</sup>。因此为了提高成像质量,需要提高对比剂的剂量、浓度和流量,但是这些方法均会增加肾脏的负担,甚至发生病变,同时辐射剂量会增加患者疾病治疗的难度,因此如何在不增加对比剂使用量的前提下提高成像质量成为研究热点<sup>[16]</sup>。能谱 CT 根据物质对 X 线吸收程度不同,进行疾病的鉴别,具有干扰因素少、使用方便、辨识度和灵敏度高等优

点,能谱 CT 作为一项崭新的 CT 成像技术,自 2009 年问世以来,已广泛应用于全身各系统疾病检查之中<sup>[17-19]</sup>。

本研究结果显示,B 组 CT 值、噪声值及 SNR 均高于 A 组,而 CTDIvol、DLP 和 ED 均显著低于 A 组( $P<0.05$ )。随着 ASIR 值的增加,图像的 SNR 随之增加,但是整体图像效果并不是 ASIR 值越大越好,过高的 ASIR 本身会引起图像的模糊效应<sup>[20]</sup>。宝石能谱 CT GSI 扫描模式较常规扫描模式有效辐射剂量降低 50% 左右,但图像质量并不受影响。即在一定体重范围内利用最佳 ASIR 成像能够在大幅度降低辐射剂量的同时保证图像质量达到诊断及鉴别诊断的要求<sup>[21]</sup>。上述结果说明宝石能谱 CT GSI 成像的效果更佳,主要是由于常规 CT 扫描是在 80~140 kVp 之间选择管电压获得混合能量的 X 线,衰减后,计算 X 射线的衰减系数,最终得到图像<sup>[22-24]</sup>,而宝能 CT 能谱同向采集单源瞬时双管电压,能够同时观察到混合能量图像和多个单能量图像,计算单个能量点组织对 X 线的衰减系数,

得到 CT 值, 观察 CT 值与能量变化的关系, 不同物质间能量变化在低能量段更明显, 因此低能量的 X 线能量接近高原子序数的物质, 增强光电效应和 CT 值, 另外低能量的 X 线穿透力弱, 接收到的原子数目下降, 增加噪声, 导致图像噪声随着能量变化而变化<sup>[25,26]</sup>。ASIR 技术建立系统噪声模型, 采用迭代的方法抑制, 使得图像更清晰, 图像处理速度更快<sup>[27-29]</sup>, 在上腹部肝脏成像中 50% ASIR 既可以降低图像噪声, 又不会对图像产生模糊效应, 图像质量达到最佳, 提示上腹部最佳权重为 50%<sup>[30]</sup>。本研究的不足: 收集样本容量少, 有待进一步扩大样本量来论证研究结果的可靠性; 本研究的患者基本为中等体型患者, 对于瘦小患者的扫描有待进一步研究。

综上所述, 在一定 BMI 范围内利用能谱 CT GSI 扫描模式及最佳 ASIR 成像能够在大幅度降低辐射剂量的同时保证图像质量达到诊断及鉴别诊断的要求, 可在临床腹部常规体检及血管成像方面应用推广。

#### 参考文献(References)

- [1] 赵晶, 徐飞, 李晓璐, 等. 不同水平的自适应统计迭代重建(ASiR)算法在能谱 CT 门静脉成像中的图像质量比较 [J]. 临床放射学杂志, 2016, 35(2): 282-287  
Zhao Jing, Xu Fei, Li Xiao-lu, et al. Comparison of Portal Vein Image Quality with Spectrum CT Based on Different Levels of Adaptive Statistical Iterative Reconstruction Algorithm (ASiR)[J]. Journal of Clinical Radiology, 2016, 35(2): 282-287
- [2] Yang J, Yang X, De Cecco CN, et al. Iterative reconstruction improves detection of in-stent restenosis by high-pitch dual-source coronary CT angiography[J]. Sci Rep, 2017, 7(1): 6956
- [3] Han H, Gao H, Xing L. Low-dose 4D cone-beam CT via joint spatiotemporal regularization of tensor framelet and nonlocal total variation[J]. Phys Med Biol, 2017, 62(16): 6408-6427
- [4] Tsutsumi Y, Fukuma S, Tsuchiya A, et al. Computed tomography during initial management and mortality among hemodynamically unstable blunt trauma patients: a nationwide retrospective cohort study [J]. Scand J Trauma Resusc Emerg Med, 2017, 25(1): 74
- [5] Lee S, Kwon H, Cho J. The Detection of Focal Liver Lesions Using Abdominal CT: A Comparison of Image Quality Between Adaptive Statistical Iterative Reconstruction V and Adaptive Statistical Iterative Reconstruction[J]. Acad Radiol, 2016, 23(12): 1532-1538
- [6] 李辉. 宝石能谱 CT 对辨别中央型肺癌与阻塞性肺实变的诊断价值 [J]. 陕西医学杂志, 2017, 46(4): 440-441  
Li Hui. The diagnostic value of gem spectrum CT in identifying central lung cancer and obstructive pulmonary consolidation [J]. Shaanxi Medical Journal, 2017, 46(4): 440-441
- [7] Weir VJ, Zhang J, Bruner AP. Dosimetric characterization and image quality evaluation of the AIRO mobile CT scanner [J]. J Xray Sci Technol, 2015, 23(3): 373-381
- [8] 方鑫, 刘义军, 刘爱连, 等. 能谱 CT GSI 扫描不同材质试管对水 CT 值及水(碘)浓度值影响的模体研究[J]. 放射学实践, 2016, 31(9): 853-856  
Fang Xin, Liu Yi-jun, Liu Ai-lian, et al. GSI phantom study with using test tubes made by different materials for the impact on the CT value of water and water-iodine concentration[J]. Radiologic Practice, 2016, 31(9): 853-856
- [9] Trattner S, Chelliah A, Prinsen P, et al. Estimating Effective Dose of Radiation From Pediatric Cardiac CT Angiography Using a 64-MDCT Scanner: New Conversion Factors Relating Dose-Length Product to Effective Dose[J]. AJR Am J Roentgenol, 2017, 208(3): 585-594
- [10] 白利杰, 黄江, 沈美诚, 等. CT 对于肝脏良性占位性病变及肝癌的鉴别诊断价值分析[J]. 现代生物医学进展, 2017, 17(4): 742-745  
Bai Li-jie, Huang Jiang, Shen Mei-cheng, et al. Clinical Value of CT in Differential Diagnosis of Liver Benign Lesion and Liver Cancer[J]. Progress in Modern Biomedicine, 2017, 17(4): 742-745
- [11] Flottmann F, Broocks G, Faizy TD, et al. CT-perfusion stroke imaging: a threshold free probabilistic approach to predict infarct volume compared to traditional ischemic thresholds [J]. Sci Rep, 2017, 7(1): 6679
- [12] Manna C, Silva M, Cobelli R, et al. High-pitch dual-source CT angiography without ECG-gating for imaging the whole aorta: intraindividual comparison with standard pitch single-source technique without ECG gating[J]. Diagn Interv Radiol, 2017, 23(4): 293-299
- [13] Wang T, Gong Y, Shi Y, et al. Feasibility of dual-low scheme combined with iterative reconstruction technique in acute cerebral infarction volume CT whole brain perfusion imaging [J]. Exp Ther Med, 2017, 14(1): 163-168
- [14] 朱正, 赵心明, 周纯武. 宝石能谱单能量成像及自适应统计迭代重建技术在腹部低剂量 CT 扫描中的可行性研究[J]. 放射学实践, 2017, 32(4): 418-422  
Zhu Zheng, Zhao Xin-ming, Zhou Chun-wu. Feasibility study of gemstone spectral imaging and adaptive statistical iterative reconstruction technique in low radiation dose abdominal CT scan [J]. Radiologic Practice, 2017, 32(4): 418-422
- [15] Schüller S, Sawall S, Stannigel K, et al. Segmentation-free empirical beam hardening correction for CT[J]. Med Phys, 2015, 42(2): 794-803
- [16] Gupta SK, Trethewey S, Brooker B, et al. Radionuclide bone scan SPECT-CT: lowering the dose of CT significantly reduces radiation dose without impacting CT image quality [J]. Am J Nucl Med Mol Imaging, 2017, 7(2): 63-73
- [17] Wang XP, Wang B, Hou P, et al. Screening and comparison of polychromatic and monochromatic image reconstruction of abdominal arterial energy spectrum CT[J]. J Biol Regul Homeost Agents, 2017, 31(1): 189-194
- [18] Yao Y, Ng JM, Megibow AJ, et al. Image quality comparison between single energy and dual energy CT protocols for hepatic imaging [J]. Med Phys, 2016, 43(8): 4877
- [19] Otrakji A, Digumarthy SR, Lo Gullo R, et al. Dual-Energy CT: Spectrum of Thoracic Abnormalities[J]. Radiographics, 2016, 36(1): 38-52
- [20] 相爱华, 固荣耀, 杨蕾, 等. 宝石能谱 CT 自适应统计迭代重建技术在儿童副鼻窦扫描中的应用[J]. 山东医药, 2017, 57(4): 59-61  
Xiang Ai-hua, Dun Rong-yao, Yang Lei, et al. Application of gem spectrum CT adaptive statistical iterative reconstruction technique in paranasal sinus scanning of children [J]. Shandong Medical Journal, 2017, 57(4): 59-61
- [21] 陈奕男, 秦将均, 覃群, 等. 宝石能谱 CT 冠脉成像在隐匿型冠心病冠状动脉粥样斑块性质判断中的价值[J]. 现代生物医学进展, 2016, 16(11): 2159-2161  
Chen Yi-nan, Qin Jiang-jun, Qin Qun, et al. Value of gem spectrum CT coronary angiography in the diagnosis of coronary atherosclerotic plaque in patients with latent coronary heart disease [J]. Progress in Modern Biomedicine, 2016, 16(11): 2159-2161 (下转第 2941 页)

- [23] Liang Y, Chang C, Zhu H, et al. Correlation between decrease of CRP and resolution of airway inflammatory response, improvement of health status, and clinical outcomes during severe acute exacerbation of chronic obstructive pulmonary disease[J]. Internal&Emergency Medicine, 2015, 10(6): 1-7
- [24] 李朔, 孟新. hs-CRP 和 IL-6 水平与急性冠状动脉综合征临床诊断相关性研究[J]. 中国实用医药, 2014, 9(1): 113-114  
Li Shuo, Meng Xin. Correlation between hs-CRP, IL-6 levels and clinical diagnosis of acute coronary syndrome [J]. China Practical Medical, 2014, 9(1): 113-114
- [25] 韩世华. 急性冠状动脉综合征患者 CD40L, TNF- $\alpha$ , IL-6 及 hs-CRP 水平与室性心律失常相关性研究[J]. 中国现代医药杂志, 2016, 18(5): 57-59  
Han Shi-hua. Correlation of CD40L, TNF- $\alpha$ , IL-6 and hs-CRP levels with ventricular arrhythmia in patients with acute coronary syndrome [J]. Modern Medicine Journal of China, 2016, 18(5): 57-59
- [26] 陈洪涛, 苗永国, 候文华, 等. 负荷量阿托伐他汀对 ACS 行 PCI 治疗患者心肌灌注、炎症因子及血管内皮功能的影响 [J]. 安徽医药, 2014, 18(12): 2375-2377  
Chen Hong-tao, Miao Yong-guo, Hou Wen-hua, et al. Effect of Atorvastatin on Myocardial Perfusion, Inflammatory Factors and Vascular Endothelial Function in ACS Patients Undergoing PCI [J]. Anhui Medical and Pharmaceutical Journal, 2014, 18(12): 2375-2377
- [27] 陆卫华, 刘晓红, 来春林. 急性冠状动脉综合征患者血浆 ETMMP-9, TNF- $\alpha$ , NO, IL-6, CRP 的变化及临床意义 [J]. 中国药物与临床, 2009, 9(2): 105-107  
Lu Wei-hua, Liu Xiao-hong, Lai Chun-lin. Changes and Clinical Significance of ETMMP-9, TNF- $\alpha$ , NO, IL-6 and CRP in Patients with Acute Coronary Syndrome[J]. Chinese Remedies and Clinics, 2009, 9(2): 105-107
- [28] 丁强, 刁奇志, 杨怀宇. 血清 Periostin、VEGF、ET-1 水平检测在急性冠状动脉综合征患者病情评估的临床价值研究[J]. 检验医学与临床, 2017, 14(9): 1297-1299  
Ding Qiang, Diao Qi-zhi, Yang Huai-yu. Clinical value of serum periostin, VEGF and ET-1 level detection in disease condition evaluation of patients with acute coronary syndrome [J]. Laboratory Medicine and Clinic, 2017, 14(9): 1297-1299
- [29] Qin H, Zhixi H U, Lin L I, et al. Effects of Xuelian Tongmai Pill on Vascular Endothelial Cell Function-Related Marker ET-1, NO and ACE in Coronary Heart Disease Mice Models with Qi Deficiency and Blood Stasis Syndrome [J]. Journal of Hunan University of Chinese Medicine, 2016, 36(2): 25-28
- [30] 田玉龙, 邢玉良, 葛中春, 等. 负荷量加高维持量阿托伐他汀对 ACS 患者介入治疗后血管内皮功能、血小板活化及炎性因子的影响[J]. 海南医学院学报, 2015, 21(02): 212-214+217  
Tian Yu-long, Xing Yu-liang, Ge Zhong-chun, et al. Influence of atorvastatinon at load dosage and high maintenance dosage on vascular endothelial function, platelet activation and inflammatory factor of patients with acute coronary syndrome after interventional therapy[J]. Journal of Hainan Medical University, 2015, 21(02): 212-214+217

(上接第 2933 页)

- [22] Wang JJ, Fan SJ, Wang LL, et al. Clinical relevance of gemstone spectral CT in the diagnosis of carotid atherosclerosis [J]. Exp Ther Med, 2017, 13(6): 2629-2636
- [23] Shinohara Y, Sakamoto M, Kuya K, et al. Carotid Plaque Evaluation Using Gemstone Spectral Imaging: Comparison with Magnetic Resonance Angiography [J]. J Stroke Cerebrovasc Dis, 2017, 26 (7): 1535-1540
- [24] Zhao Y, Wu Y, Zuo Z, et al. CT angiography of the kidney using routine CT and the latest Gemstone Spectral Imaging combination of different noise indexes: image quality and radiation dose[J]. Radiol Med, 2017, 122(5): 327-336
- [25] Wang S, Gao H, Zhang L, et al. Quasi-monochromatic imaging in x-ray CT via spectral deconvolution using photon-counting detectors [J]. Phys Med Biol, 2017, 62(6): 2208-2223
- [26] Touch M, Clark DP, Barber W, et al. A neural network -based method for spectral distortion correction in photon counting X-ray CT [J]. Phys Med Biol, 2016, 61(16): 6132-6153
- [27] Sun J, Yu T, Liu J, et al. Image quality improvement using model-based iterative reconstruction in low dose chest CT for children with necrotizing pneumonia[J]. BMC Med Imaging, 2017, 17(1): 24
- [28] Hussain FA, Mail N, Shamy AM, et al. A qualitative and quantitative analysis of radiation dose and image quality of computed tomography images using adaptive statistical iterative reconstruction [J]. J Appl Clin Med Phys, 2016, 17(3): 419-432
- [29] Zhou Z, Chen H, Wei W, et al. Low kilovoltage peak (kVp) with an adaptive statistical iterative reconstruction algorithm in computed tomography urography: evaluation of image quality and radiation dose [J]. Am J Transl Res, 2016, 8(9): 3883-3892
- [30] 殷小平, 左紫薇, 徐英进, 等. 最佳 ASIR 联合能谱单能量成像对腹部增强及血管图像质量的优化研究[J]. 临床放射学杂志, 2017, 36(2): 283-288  
Yin Xiao-ping, Zuo Zi-wei, Xu Ying-jin, et al. Optimal Adaptive Statistical Iterative Reconstruction Percentage in Monochromatic Level with Spectral CT Imaging for Improving Imaging Quality of Abdomen and Abdominal Vessels [J]. Journal of Clinical Radiology, 2017, 36(2): 283-288